The 2010 IEEE/RSJ International Conference on
Intelligent Robots and Systems
October 18-22, 2010, Taipei, Taiwan

Local Path Planning Scheme for Car-like Vehicle's Shortest Turning Motion Using Geometric Analysis

Seoung Kyou Lee, Sungon Lee, Changjoo Nam, and Nakju Lett Doh

Abstract— **This paper deals with a path planning problem for turning motion of a car-like vehicle. We propose a turning method which finds a curvature continuous optimal path between two positions for a car-like vehicle.**

This method suggests two kinds of turning case; 1) Turning path with an arc of minimum turning radius ; 2) Turning path without an arc of minimum turning radius. In each case, we derive an closed form functions, an object function and a set of related constraints. By using those equations, optimal turning path candidates corresponding to each case are made. Furthermore, we find a final distance optimal turning path among above candidates for each case.

Our algorithm is novel and more challenging compared to existing path planning algorithms in the sense that it deals more complicated problem, a turning motion. Moreover, we expect that the proposed method is helpful in various ways such as an improvement of existing path planners, like sampling based planners.

I. INTRODUCTION

To general knowledge, while a car-like vehicle have a mechanically simple steering structure compared with other kinds of vehicle such as a differently driven type, the structure of the car-like vehicle has caused several constraints related with path's curvature and have given challenging issues in generating a distance optimal path.

The firstly considered constraint of car-like path planning is a minimum turning radius caused by the length of vehicle's wheelbase. From the pioneering work by Dubins [1], several researchers ([2], [3], [4]) conducts a path planning research with this constraint. By doing so, they can generate a path closer to car-like vehicle's real motion. The path, however, does not consider curvature continuity; Rather, it contains a quantum jump of curvature in curvature profile.

Later, Kanayama [5] firstly cognates a continuous curvature problem and adopts a clothoid to overcome this problem, then numerous studies, including [6], [7] and [8], consider the continuous curvature constraint. All These algorithms have been studied under just two given configurations in an obstacle free space, so we call them a local path planner. Therefore, they can make a path connecting two configuration directly. They, however, cannot make a feasible path if an obstacle whose size is too big to avoid exists between two configurations. For this reason, they have had to be usually used with a global path planner which considers an obstacle. Moreover, those works do not evaluate distance optimality using an analytical way. Instead, some works including Shkel *et al*. [9] choose the shortest one among previously generated path set, like Dubins set. Of course, some researcher including Yang [10] solves an analytic solution for turning motion using bezier curve. The research, however, only focuses on analytic smoothness solution based on fixed way-points. In other words, the method excludes the possibility of presence of shorter path based on the way-points that move to other locations.

In this paper, we expand above works to vehicle's shortest path planning for turning motion between two arranged points with polygonal obstacle's corner. In addition, we generate a closed form functions which considers all statements mentioned above. In that, we consider 1) distance optimality, 2) obstacle avoiding turning motion, and 3) car-like vehicle's constraint. When it comes to the constraints, maximum radius of curvature and continuous curvature profile (limited curvature derivative) are reflected into the suggested planner, and to achieve it, we adopt a clothoid curve. We expect that the novel local planing method is useful not only because the method can generate a path avoiding an obstacle, but also because we can analytically analyze path's distance optimality using the closed form equations of the method.

We expect that the method can be used in various way. In fact, turning around the corner is a commonplace affair in a real world. For instance, serving vehicles in a dinning room or restaurant may have to plan a turning path to serve meals from a cuisine to a table. It also became an important issue in case of unmanned ground vehicle(UGV)'s traveling in urban area.

The algorithm can be also expected to contribute on the improvement of existing path planning algorithms. Many researchers have used a combination of supporting local path planners with various global path planners, such as Probabilistic Path Planner ([11], [7], [12], [13]) or Ariadne's Clew Algorithm ([8], [14]), to cover vehicle's kinematical constraints.

Fig. 1 shows a possible contribution of our method on PRM. Fig. 1-(a) and Fig. 1-(b) explain a road-map constructing procedure for path planning using PRM. As shown in Fig. 1-(a), PRM randomly and uniformly distributes landmarks (red cross) in free space. Each landmark consists of Euclidian coordinates and orientation at the location. Then as shown in Fig. 1-(a), each landmark evaluates a connectivity with its neighborhood using a specific local planner researched above, and then complete a road-map composed of a local planner (Fig. 1-(b)). For example, configuration 1 and 3 (2

Seoung Kyou Lee and Sungon Lee are Researcher of Korea Institute of Science and Technology, Hawolgok, Seongbuk, S. Korea dltmdrbekt@korea.ac.kr, solee@kist.re.kr

Nakju Lett Doh is an assistant professor of the school of electrical engineering, Korea University, Anamdong 5ga, Seongbuk, S. Korea nakju@korea.ac.kr

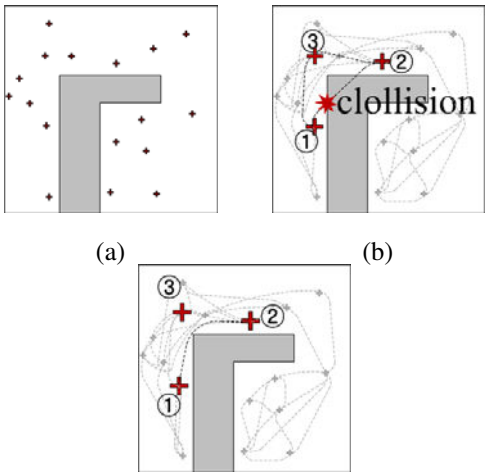

Fig. 1. Path planning procedure of Probabilistic RoadMap method and suggested method.

and 3 also) are connectable so that they can form a partial road-map while the local path connecting configuration 1 and 3 cannot be included in the road-map because of collision with an obstacle.

On the contrary, the proposed method makes possible to connect configuration 1 and 3 directly without any collision by generating a turning path (Fig. 1-(C)). Although it may lead a slight modification of orientation of 1 and 3, it will significantly reduces the length of path compared with the path through 3. Moreover, we can also compute a detailed range of consideration by using analytically generated equations.

This paper is organized as follows: In section 2, we define suggested problem more accurately and explained key concept of our strategy. Section 3 and 4 state mainly about the proceedings of equation derivation for path's length and related constraints. In final section, we discuss about simulation results, and conclding remarks follows.

II. Problem Definition and Solving Strategy

The main issue we would concern is a distance optimal turning motion given two point A and B. Fig. 2 briefly represents the problem we would focus on. In order to satisfying car-like vehicle's minimum turning radius and continuous curvature constraint, turning motion contains clothoid connecting an arc of minimum turning radius and a straight line. As stated before, most local path planner in obstacle free space constitutes a specific path set, like Dubins set, then selects the distance optimal path among the set. When it comes to turning motion, however, there cannot exist any specific feasible path set. Rather, the shape of a generated path is highly arbitrary. Hence, we choose a different strategy to get a distance optimal path. In other words, we derive closed form functions composed of an object function and related constraint functions set.

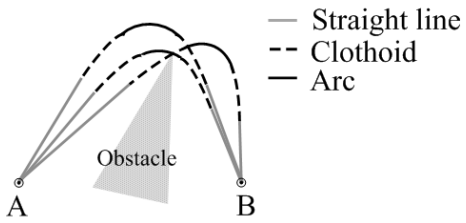

Fig. 2. Problem definition.

Object funcion ,J

An Object function denotes the length of entire turning path. It can be expressed in terms of two variables.

Constraint functions Set, Set of C

Constraint functions are derived considering geometrical relationship with an obstacle, in that these functions are derived with relative location of a generated path compared with an obstacle. Constraint functions can be expressed in terms of three variables. Two of them are used in above object function, but one additional variable is not; Thus, we need two constraint functions to eliminate the additional variable.

Here, we note that a car-like vehicle is the vehicle which can move only forward direction with constant linear velocity. On top of that, the vehicle has a maximum steering speed in that constant steering speed. It is based on the verification in [15] and [16] that generated path can be distance optimal only when steering wheel rotates with maximum speed. We also state that all clothoid pairs have the symmetrical shape because we consider a vehicle which has constant linear velocity and steering speed.

Given two point A and B, generateable feasible path can be divided into two types as shown in Fig. 3.

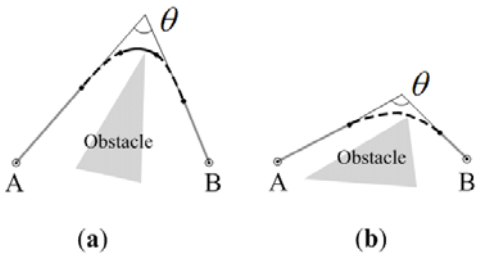

Fig. 3. Two possible path compositions. (a) A path which contains an arc with minimun turning radius. (b) A path which contains only clothoids pair.

According to the shape of a path, central angle θ between two straight line became different. If θ is enough small, the shape of the path is as shown in Fig. 3-(a). This type of path contains an arc of minimum turning radius and clothoid pair whose curvature at the end of curve is as same as the arc's

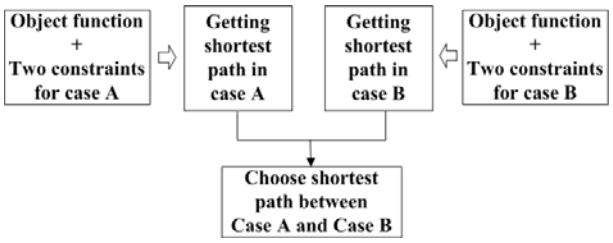

Fig. 4. Entire shortest path obtaining process. The shortest path is extracted by hierarchical process. In that, the method choose the shortest path candidate in case A and case B, than compares these candidates to select the general shortest path.

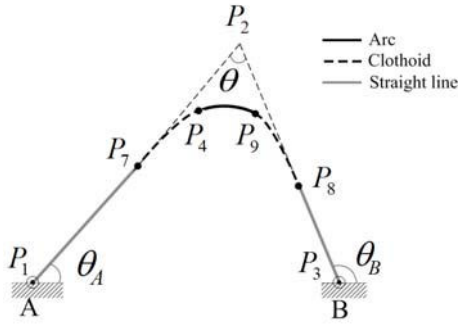

Fig. 5. Composition of the path for case A. Case A seeks for the shortest path that contains an arc of the minimum turning radius.

curvature. We name the path including the arc as Case A. In a view point of a real car-like vehicle, case A means that steering wheel is rotated completely to its limitation angle so that the car turns around with the corner with a constant curvature arc. Therefore, the entire path consists of straight line- clothoid - arc - clothoid - straight line.

On the contrary, Fig. 3-(b) shows a path whose θ is large enough. We regard this type of path as case B. This suggests that the car unwinds steering wheel as soon as wind steering wheel to certain degree of angle. Therefore, it contains no Arc. Instead, partial fragments of the complete clothoid curve used in Fig. 3-(a) are placed for turning motion because steering wheel does not wind up to its limitation angle. Therefore, entire path of this case is composed of straight line-incomplete clothoid pairs-straight line.

Then, as shown in Fig. 4, shortest turning path is obtained among the candidate shortest paths of each case A and B. In each case, shortest path candidate can be generated by combining a object function with constraint equation corresponding to the case.

This paper contains the deriving process of J and C for each cases. In section III, we will derive J_A and C_A^1, C_A^2 for case A. Then in following section (section IV), we will also derive J_B and C_B^1, C_B^2 for case B.

III. Case A: Turning path with the maximum circle

In this section, we would derive an object function J[1] and related constraints C_A^1 and C_A^2 for case A. Fig.5, describes the path we would cope with. We would express the path in terms of certain variables, θ and θ_A in the figure, where θ is the angle between two expanded line of $\overline{P_1P_7}$ and $\overline{P_3P_8}$, and θ_A (θ_B) is the angle between $\overline{P_1P_7}$ and $\overline{P_1P_3}$ ($\overline{P_3P_8}$ and $\overline{P_1P_3}$). In particular, we utilize a circumcircle with an inscribed triangle to reduce the number of related variables to achieve the purpose.

A. Object function J_A for case A

As stated in section II, object function is the length of total path, and the entire path consists of two straight lines, two clothoids and one arc in case A. Therefore, the object function can be expressed of the sum of all segments as follows

$$\begin{aligned} J_A &= \overline{P_1P_7} + clo(P_7P_5) + Arc(P_5P_9) \\ &+ clo(P_9P_8) + \overline{P_3P_8}. \end{aligned} \tag{1}$$

clo denotes a clothoid which meets with an arc of minimum turning radius. Then, P_2 a freely moves in free space according to θ_A and θ_B whereas P_1 and P_2 have fixed location. Therefore, the shape of path is determined according to the location of P_2(in that, the value of θ_A and θ_B), and θ_B can be represented by θ. It means that we can express the length of path, (1), in terms of θ and θ_A.

Clothoid curves in (1), $\widehat{P_7P_5}$ and $\widehat{P_9P_8}$, are constants value, S_{clo}, because they are determined by only constant values such as mechanical limitation of steering wheel's angle or winding(unwinding) speed of steering wheel. Therefore, we narrow the field of our problem into the expression of $\overline{P_1P_7}, \overline{P_3P_8}$ and $Arc(P_5P_9)$.

1) The length of $\overline{P_1P_7} + \overline{P_3P_8}$: To get the length of $\overline{P_1P_7}$ + $\overline{P_3P_8}$, we would modify (1) into the following form.

$$\overline{P_1P_7} + \overline{P_3P_8} = \overline{P_1P_2} + \overline{P_2P_3} - (\overline{P_7P_2} + \overline{P_2P_8}). \tag{2}$$

In this part, we would express all the part of (2) in terms of θ and θ_A, but it is very difficult and ambiguous to achieve it. At this point, we suggest a novel method, a Circumcircle and Inscribed triangle approach (CI approach).

Fig. 6 briefly describes the CI approach at certain location of P_2. In the figure, inscribed triangle, $\triangle P_1P_2P_3$, is enclosed by the circumcircle $P_1P_2P_3$.

- Derivation of $\overline{P_1P_2} + \overline{P_2P_3}$

To derive the length of (2), we firstly derive the length of $\overline{P_1P_2} + \overline{P_2P_3}$. Then, from $\triangle P_1O_1P_2$ and $\triangle P_3O_1P_2$ in Fig. 6, the length of $\overline{P_1P_2}$ and $\overline{P_2P_3}$ are given by

$$\overline{P_1P_2} = L_l = 2R_1\cos\theta_1, \tag{3}$$

$$\overline{P_2P_3} = L_r = 2R_1\cos\theta_2. \tag{4}$$

We have to express R_1, θ_1 and θ_2 in terms of θ and θ_A.

Firstly, we can get from Fig. 6

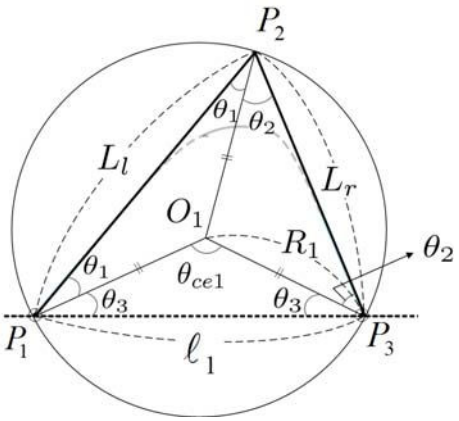

Fig. 6. CI approach for case A. Given configurations at P_1 and P_3, P_2 freely moves in free space, and constitutes a circumcircle and an inscribed triangle $\triangle P_1P_2P_3$.

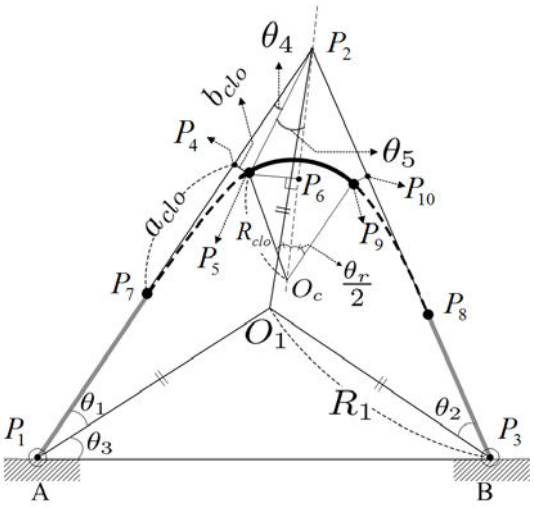

Fig. 7. Geometrical analysis for case A.

$$R_1 = \frac{\ell_1}{2\sin\theta}. \tag{5}$$

Meanwhile, we also express θ_1 and θ_2 in terms of θ and θ_A. As stated before, θ equals to $\theta_1+\theta_2$. Similarly, θ_A is also $\theta_1+\theta_3$. Then, we can derive that,

$$\theta_1 = \theta_A - \theta_3 = \theta_A - \frac{1}{2}(\pi - 2\theta) \quad , \quad \theta_1 = \theta_A + \theta - \frac{\pi}{2}, \tag{6}$$

$$\theta - \theta_2 = \theta_1 = \theta_A + \theta - \frac{\pi}{2} \quad , \quad \theta_2 = \frac{\pi}{2} - \theta_A. \tag{7}$$

$\overline{P_1P_2} + \overline{P_2P_3}$ is given by

$$L_l = \frac{\ell_1}{\sin\theta}\cos(\theta_A + \theta - \frac{\pi}{2}) = \frac{\ell_1}{\sin\theta}\sin(\theta_A + \theta), \tag{8}$$

$$L_r = \frac{\ell_1}{\sin\theta}\cos(\frac{\pi}{2} - \theta_A) = \frac{\ell_1}{\sin\theta}\sin\theta_A \tag{9}$$

, *then*

$$\begin{aligned}\overline{P_1P_2} + \overline{P_2P_3} &= L_l + L_r \\ &= \frac{\ell_1}{\sin\theta}\left[\sin(\theta_A+\theta) + \sin\theta_A\right].\end{aligned} \tag{10}$$

- Derivation of $\overline{P_7P_2} + \overline{P_2P_8}$

In previous part, we derived the length of $\overline{P_1P_2} + \overline{P_2P_3}$ in terms of θ and θ_A. Now, in this part, we would express $\overline{P_7P_2} + \overline{P_2P_8}$ in (2) in terms of those variables. Fig. 7 shows a geometric analysis to derive $\overline{P_7P_2}$ and $\overline{P_2P_8}$ in terms of θ and θ_A.

From Fig. 7, we can easily know that

$$\overline{P_7P_2} + \overline{P_2P_8} = \overline{P_4P_2} + a_{clo} + \overline{P_2P_{10}} + a_{clo}. \tag{11}$$

As mentioned in previous section, clothoid's values in case A such as a_{clo}, b_{clo} and minimum turning radius R_{clo} in Fig. 7 are all constants. Therefore, we should represent $\overline{P_4P_2}$ and $\overline{P_2P_{10}}$ in terms of θ and θ_A to derive $\overline{P_7P_2} + \overline{P_2P_8}$.

To derive $\overline{P_4P_2}$ first, we will start from the equality as follows

$$\overline{P_5P_6} = \overline{P_2P_5}\sin(\frac{\theta}{2} - \theta_4) = R_{clo}\sin\frac{\theta_r}{2}. \tag{12}$$

By adopting the formula of sin, the left side of (12) can be modified as

$$\begin{aligned}\overline{P_2P_5}\sin(\frac{\theta}{2} - \theta_4) &= \sin\frac{\theta}{2}\overline{P_2P_5}\cos\theta_4 - \cos\frac{\theta}{2}\overline{P_2P_5}\sin\theta_4 \\ &= R_{clo}\sin\frac{\theta_r}{2}.\end{aligned} \tag{13}$$

As shown in Fig. 7, $\overline{P_2P_5}\sin\theta_4$ in (13) equals to b_{clo}, and $\overline{P_2P_5}\cos\theta_4$ also equals to $\overline{P_2P_4}$.

Then we can solve (13) in terms of $\overline{P_2P_4}$ which is given by

$$\overline{P_2P_4} = \frac{1}{\sin\frac{\theta}{2}}\left[R_{clo}\sin\frac{\theta_r}{2} + \cos\frac{\theta}{2}b_{clo}\right]. \tag{14}$$

By symmetric property, we can easily confirm that $\overline{P_2P_4}$ is equal to $\overline{P_2P_{10}}$. Then by substituting (14) for $\overline{P_2P_4}$ and $\overline{P_2P_{10}}$ in (11), we can get the length of $\overline{P_1P_7}$ and $\overline{P_3P_8}$ as follows

$$\overline{P_7P_2} = \overline{P_2P_8} = \frac{1}{\sin\frac{\theta}{2}}\left[R_{clo}\sin\frac{\theta_r}{2} + \cos\frac{\theta}{2}b_{clo}\right] + a_{clo} \tag{15}$$

, then

$$\overline{P_7P_2} + \overline{P_2P_8} = \frac{2}{\sin\frac{\theta}{2}}\left[R_{clo}\sin\frac{\theta_r}{2} + \cos\frac{\theta}{2}b_{clo}\right] + 2a_{clo}. \tag{16}$$

We can also express θ_r in (16) by θ and θ_A as follows

$$\theta_r = \pi - 2\theta_{clo} - \theta. \tag{17}$$

By substituting θ_r in (17) for that in (16), we can get

$$\begin{aligned}\overline{P_7P_2}+\overline{P_2P_8} &= \frac{2}{\sin\frac{\theta}{2}}\left[R_{clo}\sin\frac{(\pi-2\theta_{clo}-\theta)}{2}+\cos\frac{\theta}{2}b_{clo}\right] \\ &+ 2a_{clo}. \end{aligned} \quad (18)$$

Now, we can get the length of $\overline{P_1P_7}+\overline{P_3P_8}$ in (2) by combining (10) and (18). After simplifying (10) and (18) by using cos/sin laws, we can get the function as follows

$$\begin{aligned}\overline{P_1P_7}+\overline{P_3P_8} &= \frac{\ell_1}{\sin\theta}\left[\sin(\theta_A+\theta)+\sin\theta_A\right] \\ &- 2a_{clo}-\frac{2}{\sin\frac{\theta}{2}}\left[R_{clo}\cos(\frac{\theta}{2}+\theta_{clo})+\cos\frac{\theta}{2}b_{clo}\right]. \end{aligned} \quad (19)$$

2) The length of Arc (P_5P_9): The length of Arc (P_4P_9) is very simple. We already derive θ_r in terms of θ and θ_A in (17). Therefore, we can get the length as follows

$$\begin{aligned}Arc(P_5P_9) &= \theta_r R_{clo} \\ &= R_{clo}(\pi-2\theta_{clo}-\theta). \end{aligned} \quad (20)$$

3) Derivation of Object function J_A: Now, we got all segments of (1). By combining (19), (20) and two complete clothoid segments, we can complete the object function J_A for case A as follows

$$\begin{aligned}J_A &= \overline{P_1P_7}+clothoid(P_7P_5)+Arc(P_5P_9)+clothoid(P_9P_8)+\overline{P_3P_8} \\ &= \frac{\ell_1}{\sin\theta}\left[\sin(\theta_A+\theta)+\sin\theta_A\right]+2S_{clo} \\ &- 2a_{clo}-\frac{2}{\sin\frac{\theta}{2}}\left[R_{clo}\cos(\frac{\theta}{2}+\theta_{clo})+\cos\frac{\theta}{2}b_{clo}\right] \\ &+ R_{clo}(\pi-2\theta_{clo}-\theta). \end{aligned} \quad (21)$$

B. Constraints for case A

In previous section, we derived the length of entire path using two variables θ and θ_A. This section derives constraints C_A^1 and C_A^1. Like the path 4 in Fig. 8, the derivation of constraints are based on the assumption that the shortest path exists only when some part of the path places slightly near obstacle's corner P_{11}. We can show that the length of any outer path, like 5, is longer than 4 by conducting simple MATLAB simulation. We, however, do not denote it because of page limitation.

On top of that, the location among the path causes an additional variable. Therefore, there are two constraints in each case, and one of the constraints is used to reduce the number of variables of all constraint equations (from three to two variables).

Finally, there exists two kinds of constraints set in case A; 1) Constraint set 1 for the case when corner places on path's clothoid segments (C_{A-1}^1 and C_{A-1}^2). 2) Constraint set 2 for the case when corner places on path's arc (C_{A-2}^1 and C_{A-2}^2). Each constraint set are used with the object function J_A separately, and the distance optimal path in case A is obtained among constraint set 1 and 2. The constraint set 1 and 2 is derived in following subsection.

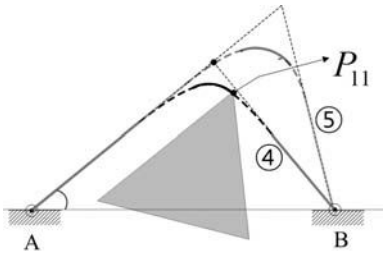

Fig. 8. The change of guideline going with increasing θ. When P_2' goes to P_1 closer, the former triangle and the path always enclose the latter.

1) Base Triangle: As mentioned in section II, constraints are derived by using the relationship with obstacle's geometrical feature. In this regard, we would firstly define a base triangle. It is the triangle which connects the point A, B and obstacle's vertex (or via-point). For example, $\triangle P_1P_3P_{11}$ in Fig. 8 is a base triangle. By using this triangle, we can derive two constraints which tell about its adjoining path is the shortest path according to an object function.

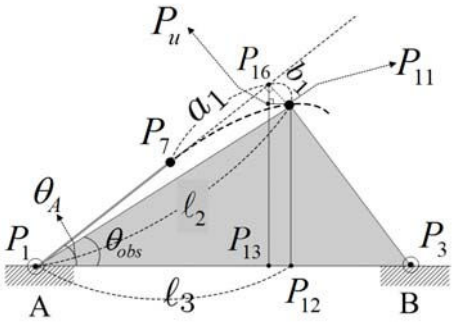

Fig. 9. Geometric analysis for constraint A-1.

2) Constraints Set 1 (C_{A-1}^1, C_{A-1}^2) : Vertex contacts with the point on clothoid: Fig.9 shows the relationship between variables when point P_{11} contacts with a left clothoid of the path. θ_{obs} is constant value because A, B andn P_{11} are given points. However, clothoid related values a_1 (x-axis projection value) and b_1 (y-axis projection value) are not constant. Instead, they varies according to which part of clothoid contact with corner. In fact, by equation (4) in Kostov's research [17] about clothoid, a_1 and b_1 are all the function of another clothoid parameter t_1 (like 't' in [17]). This parameter is the third variable of this constraint set.

- Derivation of constraint C_{A-1}^1

From $\triangle P_1P_{11}P_{16}$ in Fig. 9 we can easily get the constraint C_{A-1}^1 which is given by

$$\ell_2\sin(\theta_A-\theta_{obs})=b_1, \quad (22)$$

By adopting clothoid's Y-axis equation(Fresnel integral in [17]), we can express (22) in terms of θ, θ_A, and clothoid parameter t_1 as follows

$$\ell_2 \sin(\theta_A - \theta_{obs}) = \alpha \int_0^{t_1} \sin(\frac{u^2}{2}) du \tag{23}$$

where α is constant parameter which determines the shape of clothoid related with only car-like vehicle's specification. t_1, however, is a variable as mentioned in previous paragraph.

- Derivation of constraint C^2_{A-1}

Second constraint is related with the location of point A, B and obstacle's corner point $P_1$1. In other words, we would use the height of Base Triangle $P_1P_{11}P_3$ in Fig. 9. Then the fundamental relationship for the constraint C^2_{A-1} is given by

$$\overline{P_{16}P_{13}} = \overline{P_{16}P_u} + \overline{P_{11}P_{12}}. \tag{24}$$

From Base Triangle in Fig. 9, we can express $\overline{P_{11}P_{12}}$ in (24) as follow

$$\overline{P_{11}P_{12}} = \ell_2 \cos\theta_{obs}. \tag{25}$$

Then $\overline{P_{11}P_{16}}$ is perpendicular to the $\overline{P_1P_{16}}$. Therefore, $\angle P_{11}P_{16}P_u$ equals to θ_A. By using the fact, we can also represent $\overline{P_{16}P_u}$ in (25) as follow

$$\overline{P_{16}P_u} = b_1 \cos\theta_A. \tag{26}$$

Finally, the length of $\overline{P_{16}P_{13}}$ in (25) is given by

$$\begin{aligned} \overline{P_{16}P_{13}} &= \overline{P_1P_{16}} \sin\theta_A = (\overline{P_1P_7} + \overline{P_7P_{16}}) \sin\theta_A \\ &= (\overline{P_1P_2} - \overline{P_7P_2} + \overline{P_7P_{16}}) \sin\theta_A = (eq(8) - eq(15) + a_1)) \sin\theta_A \end{aligned} \tag{27}$$

Then it can be

$$\left[\frac{\ell_1}{\sin\theta}\sin(\theta_A+\theta) - \frac{1}{\sin\frac{\theta}{2}}\left[R_c \sin\frac{\theta_r}{2} + \cos\frac{\theta}{2} b_{clo}\right] - a_{clo} + a_1\right] \sin\theta_A. \tag{28}$$

Then by substituting (25), (26), and (28) for corresponding symbols in (24), we can derive constraint C^2_{A-1} as follow

$$\begin{aligned} &(\frac{\ell_1}{\sin\theta}\sin(\theta_A+\theta) - \frac{1}{\sin\frac{\theta}{2}}\left[R_c\cos(\theta_{clo}+\frac{\theta}{2}) + \cos\frac{\theta}{2} b_{clo}\right] \\ &\quad - a_{clo} + a_1) \sin\theta_s = b_1 \sin(\frac{\pi}{2} - \theta_s) + \ell_2 \sin\theta_{obs}. \end{aligned} \tag{29}$$

where a_1 and b_1 are functions in terms of t_1 by the clothoid's property. Therefore, (29) is also the function of θ, θ_A and t_1.

3) Constraints Set 2 (C^1_{A-2}, C^2_{A-2}) : Vertex contacts with the point on Arc of maximum curvature: Fig. 10 describes the constraint set 2. Similar with constraint set 1, constraint set 2 also contains an additional variable which denotes the location of obstacle's corner on the Arc of path. While t_1 played a role as an additional variable for the constraints set 1, θ_r^* in Fig. 10 is a key variable in this case. In that, two constraints in this case will be expressed in terms of θ, θ_A and θ_r^*. Then by combining two constraints with J_A, one of those variables will be eliminated.

- Derivation of constraint C^1_{A-2}

The procedure to derive constraint C^1_{A-2} is similar with constraint C^1_{A-1}.

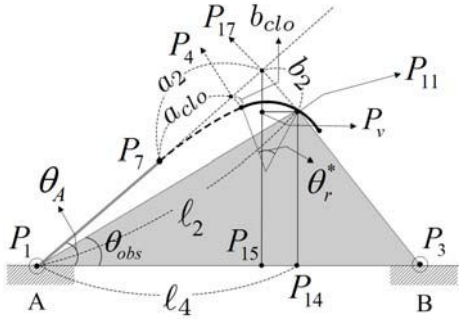

Fig. 10. Geometric analysis for constraint A-2.

From $\triangle P_1P_{11}P_{17}$ in Fig. 10, we can also say that

$$\ell_2 \sin(\theta_A - \theta_{obs}) = b_2, \tag{30}$$

Then, to represent the variable b_2 in terms of θ_r^* and other given variables, we draw a additional dashed line $\overline{O_cQ}$ parallel with $\overline{P_{11}P_{18}}$ or $\overline{P_{11}P_{19}}$ as shown in Fig.11. Then the equation of b_2 is given like,

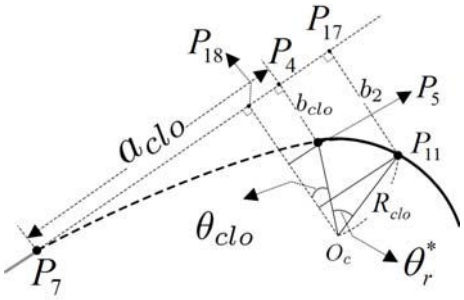

Fig. 11. Obtaining b_2 in terms of other variables.

$$b_2 = b_{clo} + R_{clo}\cos\theta_{clo} - R_{clo}\cos(\theta_r^* + \theta_{clo}). \tag{31}$$

By substituting b_2 in (31) for that in (30), we can get a constraint equation C^1_{A-2} which is given by

$$\ell_2 \sin(\theta_A - \theta_{obs}) = b_{clo} + R_{clo}\cos\theta_{clo} - R_{clo}\cos(\theta_r^* + \theta_{clo}). \tag{32}$$

- Derivation of constraint C^2_{A-2}

Constraint C^2_{A-2} is also start from the relationship using the height of base triangle $\triangle P_{11}P_1P_3$ in Fig. 10. The fundamental relationship of this constraint is like,

$$\overline{P_{17}P_{15}} = \overline{P_{17}P_v} + \overline{P_{11}P_{14}} \tag{33}$$

We will transform above relation (33) to the function of θ, θ_A and θ_r^*. To achieve it, we firstly have to get the length of $\overline{P_{11}P_{14}}$. From the $\triangle P_1P_{11}P_{14}$, we can get

$$\overline{P_{11}P_{14}} = \ell_2 \cos\theta_{obs}. \quad (34)$$

When it comes to $\overline{P_{17}P_v}$, we can get also

$$\overline{P_{17}P_v} = b_2 \cos\theta_A. \quad (35)$$

By substituting b_2 in (31) for that in (35), we can get

$$\overline{P_{17}P_v} = (b_{clo} + R_{clo}\cos\theta_{clo} - R_{clo}\cos(\theta_r^* + \theta_{clo}))\cos\theta_A. \quad (36)$$

Finally, we can get the length of $\overline{P_{17}P_{15}}$ in (33) as follows

$$\overline{P_{17}P_{15}} = \overline{P_1P_{17}}\sin\theta_A, \quad (37)$$

where $\overline{P_1P_{17}}$ is given by

$$\begin{aligned}\overline{P_1P_{17}} &= \overline{P_1P_4} + \overline{P_7P_{17}} = \overline{P_1P_2} - \overline{P_7P_2} + \overline{P_7P_{17}} \\ &= eq(8) - eq(15) + a_{clo} + \overline{P_{18}P_{19}}. \end{aligned} \quad (38)$$

Therefore, $\overline{P_{17}P_{15}}$ in (37) is as follow

$$\left[\frac{\ell_1}{\sin\theta}\sin(\theta_A+\theta) - \frac{1}{\sin\frac{\theta}{2}}\left[R_{clo}\cos(\frac{\theta}{2}+\theta_{clo}) + b_{clo}\cos\frac{\theta}{2}\right]\right]\sin\theta_A + [R_c(\sin(\theta_{clo}+\theta^*) - \sin\theta_{clo})]\sin\theta_A. \quad (39)$$

Then by substituting $\overline{P_{17}P_{15}}$ in (39), $\overline{P_{17}P_v}$ in (36) and $\overline{P_{11}P_{14}}$ in 34 for those in (33), we can get a constraint C^2_{A-2} which is given by

$$\begin{aligned}&\left[\frac{\ell_1}{\sin\theta}\sin(\theta_A+\theta) - \frac{1}{\sin\frac{\theta}{2}}\left[R_c\sin\frac{\pi-2\theta_{clo}-\theta}{2} + \cos\frac{\theta}{2}b_{clo}\right]\right]\sin\theta_A \\ &+R_c(\sin(\theta_{clo}+\theta^*) - \sin\theta_{clo})\sin\theta_A \\ &-[b_{clo} + R_c(\cos\theta_{clo} - \cos(\theta^*+\theta_{clo}))]\sin(\frac{\pi}{2}-\theta_A) \\ &-\ell_2\sin\theta_{obs} = 0. \end{aligned} \quad (40)$$

IV. Case B: turning path without the maximum circle

In this section, we consider the path composed of only two straight lines and two clothoids. This case occurs when a vehicle do not need to rotate a corner with maximum turning radius.

Principles and process to derive an object function J_B and related constraints C^2 are as same as the process of case A. Because of the page limitation, we would state the closed form result for case B directly.

Object function J_B for case B

$$\begin{aligned}J_B &= \frac{\ell_1}{\sin\pi - {t_2}^2}\left[\sin(\theta_A + \pi - {t_2}^2) + \sin(\theta_A)\right] - 2a_3 \\ &+ \frac{2b_3}{\tan\frac{\pi-{t_2}^2}{2}} + 2\alpha(\pi - {t_2}^2), \end{aligned} \quad (41)$$

Constraints for case B, C^1_B and C^2_B

$$\ell_2\sin(\theta_A - \theta_{obs}) = b_4, \quad (42)$$

$$\left[\frac{\ell_1}{\sin(\pi-{t_2}^2)}\cos(\theta_A - {t_2}^2 + \frac{\pi}{2}) - a_3 - \frac{b_3}{\tan\frac{\pi-{t_2}^2}{2}} + a_4\right]\sin\theta_A - b_4\sin(\frac{\pi}{2} - \theta_{obs}) = \ell_2\sin\theta_{obs}, \quad (43)$$

where a_3, a_4, b_3 and b_4 are clothoid related variables that can be represented by clothoid parameters, t (We call the parameter for a_3 and b_3 as t_2 and t_3 for a_4 and b_4). The variables in case B are slightly different from case A. In other words, (41), (42) and (43) are the function in terms of θ_A, t_2 and t_3.

V. Simulation result

In order to conduct simulation for suggested algorithm, we assumed a car-like vehicle whose body length is 4.9m long cargo unmanned vehicle with 4.96m/s line velocity, 14.32m of Maximum turning radius and $\frac{\pi}{9}$(rad/s) of Steering Wheel's Angular Velocity. In addition, the vehicle can only move forward direction. Then from vehicle's specification, we can calculate clothoid's shape in out simulation according to clochoid equations. Calculated specification of clothoid is that τ_{clo} is 0.414 and α is 11.96.

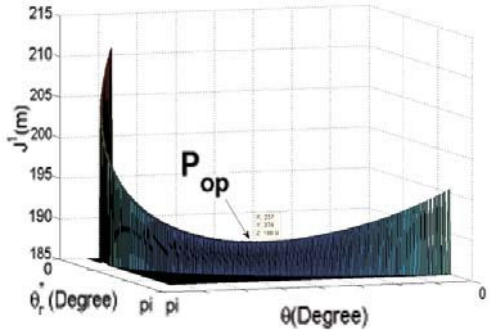

Fig. 12. Estimated distance optimal path from simulation result of case A.

Fig. 12 presents the simulation result for the length of entire path (Object function J_A with C^1_{A-2} and C^2_{A-2}). Arrowed point P_{op} is the distance optimal path. Z-axis values (J values) of P_{op} is lower than any other points. All points in case for J_A with C^1_{A-1} and C^2_{A-1} are found that they are longer than P_{op}. In addition, all possible path in case B is revealed that it is not feasible. We cannot state the figures of lateral two case (J with C^1_{A-1}, C^2_{A-1} and case B) because of page limitation.

Fig. 13 shows a visible path generated according to the P_{op}. All variables of P_{op} are stated. In the figure, we can confirm that $\theta = 68.91^o$, $\theta_r^* = 34.5^o$ is , and $\theta_A = 58.68^o$.

We compared the path generated by our method with a path generated by an existing local-global concatenated planner using MATLAB simulation and drawing tool. Dashed gray line in Fig. 14 shows an existing method. We randomly

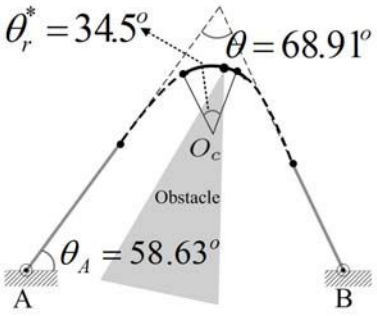

Fig. 13. Estimated distance optimal path from simulation result of case A.

pointed in the map, and link it according to exiting way by using drawing tool. On the contrary, colored path is the proposed method. The line was the result of MATLAB simulation. The length of our method is 189.9m while the existing method shows 237.3m. It is 20 percent shorter than the existing method.

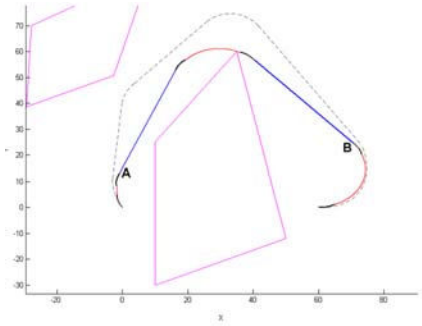

Fig. 14. Local path implementation simulation into global path planner.

VI. CONCLUSIONS

In this paper, we propose a direct approach that generate a feasible shortest path for a car-like vehicle with a constant linear and angular velocity. An object function that describes the length of a path is derived and related constrains that reduce the searching region in the solution space is suggested.

With the proposed object function, we can generate a feasible shortest path for a case when the maximum circle does not appear during a turning period, then

Although a set of complete closed form functions is derived, the analytic solution is not yet found. Our future work is to find an analytic solution which generates the feasible shortest path in a constant time.

ACKNOWLEDGEMENT

This work was supported (in part) by Ministry of Knowledge Economy under Human Resources Development Program for Convergence Robot Specialists.

REFERENCES

[1] L. E. Dubins, "On curves of minimal length with a constraint on average curvature, and with prescribed initial and terminal positions and tangents," *American Journal of Mathematics*, vol. 79, no. 3, pp. 497–516, 1957.

[2] uh Nam Bui, P. Soukres, J. D. Boissonnat, and J. P. Laumond, "Smooth local path planning for autonomous vehicles," in *International Conference on Robotics and Automation*, pp. 2–7, 1994.

[3] J. A. Reeds and L. A. Shepp, "Trajectory optimal paths for a car that goes both forwards and backwards," *Paciffic Journal of Mathematics*, vol. 145, no. 2, pp. 367–393, 1990.

[4] G. Desaulniers and F. Soumis, "An efficient algorithm to find a shortest path for a car-like robot," *IEEE Trans. on Robotics and Automation*, vol. 11, no. 6, pp. 819–828, 1995.

[5] Y. Kanayama and N. Miyake, "Trajectory generation for mobile robots," in *Robotics Research*, vol. 3, pp. 333–340, Cambridge: MA: MIT Press, 1986.

[6] S. S. Weerakamhaeng Yossawee, Takashi Tsubouchi and S. Yuta, "Path generation for articulated steering type vehicle using symmetrical clothoid," in *IEEE Int. Conf. on Information and Technology*, pp. 187–192, 2002.

[7] F. Lamiraux and J.-P. Laumond, "Smooth motion planning for car-like vehicles," *IEEE Trans. on Robotics and Automation*, vol. 17, no. 4, pp. 498–502, 2001.

[8] A. Scheuer and T. Fraichard, "Planning continuous-curvature paths for car-like robots," in *Proc. of IEEE/RSJ Int. Conf. on Intelligent Robots and Systems*, pp. 1304–1311, 1996.

[9] A. M. Shkel and V. J. Lumelsky, "On calculation of optimal paths with constrained curvature: The case of long paths," in *International Conference on Robotics and Automation*, pp. 3578–3583, 1996.

[10] K. Yang and S. Sukkarieh, "An analytical continuous-curvature path-smoothing algorithm," *IEEE Trans. on Robotics*, vol. 26, no. 3, pp. 561–568, 2010.

[11] P. Svestka and M. H. Overmars, "Probabilistic path planning," *Lecture Note in Computer Science*, vol. 229, pp. 255–304, 1998.

[12] L. Kavraki, P. Svestka, J.-C. Latombe, and M. H. Overmars, "Probabilistic roadmaps for path planning in high dimensional configuration spaces," *IEEE Trans. on Robotics and Automation*, vol. 12, pp. 566–580, 1996.

[13] G. Song and N. M. Amato, "Randomized motion planning for car-like robots with c-prm," in *Proc. of IEEE/RSJ Int. Conf. on Intelligent Robots and Systems*, pp. 37–42, 2001.

[14] A. Scheuer and T. Fraichard, "From reeds and shepp's to continuous-curvature paths," *IEEE Trans. on Robotics*, vol. 20, no. 6, pp. 1025–1035, 2004.

[15] A. Scheuer and C. Laugier, "planning sub-optimal and continuous curvature paths for car-like robots," in *Proc. of IEEE/RSJ Int. Conf. on Intelligent Robots and Systems*, pp. 1–7, 1998.

[16] J.-D. Boissonnat, A. Cerezo, and J. Leblond, "a note on shortest paths in the plane subject to a constraint on the derivative of the curvature," inria-0074512, INRIA, 1994.

[17] V. Kostov and E. Degtiariova-Kostova, "Some properties of clothoids," inria-00073940, INRIA, December 1995.